The [3]He flux gauge in the Sargasso Sea: a determination of physical nutrient fluxes to the euphotic zone at the Bermuda Atlantic Time-series Site

R. H. R. Stanley[1], W. J. Jenkins[2], S. C. Doney[2], and D. E. Lott III[2]

[1]Department of Chemistry, Wellesley College, Wellesley, MA 02481, USA
[2]Department of Marine Chemistry, Woods Hole Oceanographic Institution, Woods Hole, MA 02543, USA

Correspondence to: R. H. R. Stanley (rachel.stanley@wellesley.edu)

Abstract. Significant rates of primary production occur in the oligotrophic ocean, without any measurable nutrients present in the mixed layer, fueling a scientific paradox that has lasted for decades. Here, we provide a new determination of the annual mean physical supply of nitrate to the euphotic zone in the western subtropical North Atlantic. We combine a 3-year time series of measurements of tritiugenic [3]He from 2003 to 2006 in the surface ocean at the Bermuda Atlantic Time-series Study (BATS) site with a sophisticated noble gas calibrated air–sea gas exchange model to constrain the [3]He flux across the sea–air interface, which must closely mirror the upward [3]He flux into the euphotic zone. The product of the [3]He flux and the observed subsurface nitrate–[3]He relationship provides an estimate of the minimum rate of new production in the BATS region. We also apply the gas model to an earlier time series of [3]He measurements at BATS in order to recalculate new production fluxes for the 1985 to 1988 time period. The observations, despite an almost 3-fold difference in the nitrate–[3]He relationship, yield a roughly consistent estimate of nitrate flux. In particular, the nitrate flux from 2003 to 2006 is estimated to be $0.65 \pm 0.14\,\mathrm{mol\,m^{-2}\,yr^{-1}}$, which is $\sim 40\,\%$ smaller than the calculated flux for the period from 1985 to 1988. The difference in nitrate flux between the time periods may be signifying a real difference in new production resulting from changes in subtropical mode water formation. Overall, the nitrate flux is larger than most estimates of export fluxes or net community production fluxes made locally for the BATS site, which is likely a reflection of the larger spatial scale covered by the [3]He technique and potentially also by the decoupling of [3]He and nitrate during the obduction of water masses from the main thermocline into the upper ocean. The upward nitrate flux is certainly large enough to support observed rates of primary production at BATS and more generally in the oligotrophic subtropical ocean.

1 Introduction

Primary production in the subtropical oligotrophic gyres has been an active area of study for decades. In particular, scientists have long puzzled over the seemingly paradoxical drawdown of summertime dissolved inorganic carbon despite no visible source of nutrients (Michaels et al., 1994). Numerous studies using geochemical tracers, sediment traps, and bottle incubations have been performed at the Bermuda Atlantic Time-series Study (BATS) site over the past several decades (e.g., Brew et al., 2009; Jenkins and Doney, 2003; Jenkins and Goldman, 1985; Spitzer and Jenkins, 1989; Gruber et al., 1998; Stanley et al., 2012; Stewart et al., 2011; Buesseler et al., 2008; Maiti et al., 2009, 2012; Owens et al., 2013; Lomas et al., 2010) in order to quantify various aspects of biological production and to shed light on this enigma. Floating sediment traps give a direct measure of export production but may be biased by collection efficiency due to hydrodynamic biases and swimmers (Buesseler, 1991), as well as by the limited amount of time they are in the water. Bottle incubations, although primarily used to determine net primary production (Marra, 2002, 2009), can also be conducted to give determinations of new production when conducted with

^{15}N (Dugdale et al., 1992). Bottle incubations give useful information but may be limited by the so-called bottle effects of constraining organisms to a bottle (Peterson, 1980; Harrison and Harris, 1986; Scarratt et al., 2006). Geochemical tracers give large-scale averages of the rates of new production, net community production, or export production. These rates, however, can be difficult to interpret since quantitative interpretation of the tracer data often depends on estimates of physical transport. Thus, it is useful to calculate rates of production using numerous approaches and to compare them.

One approach that has been used before in the Sargasso Sea is to estimate a lower bound of new production by calculating the upward physical nutrient flux (Jenkins and Doney, 2003; Jenkins, 1988b). The global inventory of natural tritium has been dwarfed by the production of so-called "bomb tritium" that was created during the atmospheric nuclear weapons tests in the 1950s and 1960s (Weiss and Roether, 1980). This tritium was deposited in large part in the Northern Hemisphere (Doney et al., 1992; Stark et al., 2004) and has subsequently entered the oceanic thermocline and abyss by subduction, water mass formation, mixing, and advection (e.g., Rooth and Ostlund, 1972; Ostlund et al., 1974; Broecker and Peng, 1980). Tritium, which has a half-life of 12.31 years (MacMahon, 2006), decays to ^{3}He, a stable, inert, and rare isotope of helium. Over the decades since the bomb transient, a significant inventory of this isotope has accrued within the main thermocline of the North Atlantic. There is evidence of an efflux of this isotope via gas exchange from the surface ocean (Jenkins, 1988a, c). Inasmuch as this tritiugenic excess ^{3}He has a nutrient-like distribution in the thermocline – it is small in the surface ocean due to gas exchange loss and reaches a maximum within the thermocline due to in situ tritium decay – it is tempting to argue that the physical return of this isotope to the shallow ocean can be used as a "flux gauge" to determine the rate of physical nutrient supply to the euphotic zone (Jenkins, 1988a; Jenkins and Doney, 2003). Here, we report the results of a 3-year time series of helium isotope measurements taken approximately monthly between 2003 and 2006 in the surface ocean near Bermuda that allow another determination of this nutrient flux. We compare the calculated nutrient flux to the nutrient flux determined at the same location using the same method for the period of 1985 to 1998 as well as to export production fluxes calculated in the Sargasso Sea for the time period of 2003 to 2006.

2   Methods

2.1   Data collection

Samples for ^{3}He, a suite of noble gases, and tritium were collected at the BATS site (31.7° N, 64.2° W) on core BATS cruises at an approximately monthly resolution between April 2003 and April 2006. The BATS site, located in the subtropical North Atlantic, is representative of a typical oligotrophic gyre. Much biogeochemical research has occurred at that site because of the long-standing time series measurements carried out there (Lomas et al., 2013). In particular, as part of the regular time series, export fluxes are estimated monthly from surface-tethered floating and upper-ocean sediment traps (Lomas et al., 2010), and rates of net primary production are estimated monthly from radiocarbon bottle incubations (Steinberg et al., 2001). In addition, other researchers have measured export using ^{234}Th (Maiti et al., 2009), neutrally buoyant sediment traps (Owens et al., 2013), or apparent oxygen utilization rates (Stanley et al., 2012; Jenkins, 1980). Net community production has been estimated from the seasonal accumulation of O_2 / Ar (Spitzer and Jenkins, 1989) and the drawdown of dissolved inorganic carbon (Gruber et al., 1998; Brix et al., 2006; Fernandez-Castro et al., 2012). New production has been estimated from bottle incubations (Lipschultz, 2001; Lipschultz et al., 2002) and has also been studied using nitrogen isotopes (Fawcett et al., 2014; Knapp et al., 2008).

The ^{3}He and noble gas samples for this study were collected from Niskin bottles by gravity feeding through Tygon tubing into valved 90 mL stainless steel cylinders. Typically 22 samples were collected within the upper 400 m, and thus, depending on mixed-layer depth, there were usually several samples collected within the mixed layer. Within 24 h of sampling, the gas was extracted from the water stored in the cylinders into $\sim$ 30 mL aluminosilicate glass bulbs. The bulbs were then brought to the Isotope Geochemistry Facility at WHOI (Woods Hole Oceanographic Institution), where they were analyzed for ^{3}He, ^{4}He, Ne, Ar, Kr, and Xe using a dual mass spectrometric system with the ^{3}He being analyzed by a magnetic sector mass spectrometer and the other noble gases being analyzed by a quadrupole mass spectrometer (Stanley et al., 2009a). In particular, the magnetic sector mass spectrometer for ^{3}He measurements was a purpose-built, branch tube, statically operated, dual-collector instrument equipped with a Faraday cup and a pulse-counting secondary electron multiplier. Precision of the ^{3}He measurements, based on duplicates, was 0.15 %. The focus of this paper is on the ^{3}He measurements, but the other noble gases were used to calculate gas exchange fluxes (Stanley et al., 2009b), which is an important term in the calculation of ^{3}He flux from the ^{3}He data.

Samples for tritium were collected from the same Niskin bottles by gravity feeding through Tygon tubing into 500 mL argon-filled flint glass bottles, as described in Stanley et al. (2012). The tritium samples were degassed at the Isotope Geochemistry Facility at WHOI (Lott and Jenkins, 1998), and then the resulting ^{3}He ingrowth was measured on a purposefully constructed, branch tube dual-collector magnetic sector mass spectrometer (a different one than the one used above for ^{3}He samples). The resulting tritium concentrations were used to correct for tritium ingrowth in the ^{3}He samples between the time of collection and the time of measurement.

2.2 Calculation of fluxes

The nitrate flux was calculated in a similar way as described in Jenkins and Doney (2003). The most notable difference was that in this study the dynamic solubility equilibrium value of ^{3}He was modeled, taking both solubility and bubble injection into account, as described in more detail below. To calculate the nitrate flux, first a ^{3}He flux was calculated and then the slope of the nitrate : ^{3}He ratio was applied. The ^{3}He flux was calculated from the gas exchange parameterization of Stanley et al. (2009b), which was devised specifically from the noble gas samples collected at the same time as the ^{3}He samples and thus is well suited to the study site and sampling conditions. In particular, the ^{3}He flux (F_{He3}) was calculated as the product of a gas transfer velocity k, as determined in Stanley et al. (2009b), and the difference in concentration between the measured ^{3}He concentration (C) and the dynamic solubility equilibrium value (C_{eq}):

$$F_{He3} = k \times (C - C_{eq}). \qquad (1)$$

The dynamic solubility equilibrium refers to the value of δ^3He that would be observed in the ocean if the atmosphere were in equilibrium with the water. This is governed by the Henry's law constant for ^{3}He vs. ^{4}He (i.e., the fractionation associated with solubility) as well as by the fractionating effect of gas exchange, including bubble processes, on the ratio of ^{3}He and ^{4}He. Thus the dynamic solubility equilibrium is the required saturation state such that diffusive gas exchange will balance the bubble effects in a quasi-steady-state system. Laboratory experiments have determined the isotope effect in solution for helium in water as a function of temperature (Benson and Krause, 1980). Given that the helium isotope ratio may be further affected by isotopic fractionation in molecular diffusion (Bourg and Sposito, 2008) associated with the balance between wave-induced bubble trapping and air–sea exchange (Fuchs et al., 1987; Jenkins, 1988b), we have used our observations of the full suite of noble gases on these samples to develop a much more complete model of this dynamic equilibrium isotope effect. Thus, the dynamic solubility equilibrium value for ^{3}He, C_{eq}, was determined by adding ^{3}He isotopes to a one-dimensional Price–Weller–Pinkel (PWP) model (Price et al., 1986) subject to 6-hourly NCEP (National Center for Environmental Prediction) reanalysis forcing (Kalnay et al., 1996) and QuikSCAT winds from the BATS site (Stanley et al., 2006, 2009b). The model used the temperature-dependent solubility of ^{3}He from Benson and Krause (1980) and the molecular diffusivity value from Bourg and Sposito (2008). The calculated dynamic solubility equilibrium is sensitive to the amount of air injection, and thus the other noble gases were used to constrain the air injection (Stanley et al., 2009b; subsequently referred to as S09). In particular, the dynamic solubility equilibrium was calculated, including the effects of diffusive gas exchange, partially trapped bubbles, and completely trapped bubbles according to the equations below, described in full in S09.

The diffusive gas exchange flux of ^{3}He (or another gas such as ^{4}He) (in units of mol m^{-3} s^{-1}) was calculated as

$$F_{GE} = \gamma_G \cdot 8.6 \times 10^{-7} \left(\frac{Sc}{660}\right)^{-0.5} u_{10}^2 \left(C_{i,eq} - C_{i,w}\right), \qquad (2)$$

where γ_G is a first-order, tunable model parameter that scales the magnitude of diffusive gas exchange, Sc is the Schmidt number of the gas (i.e, ^{3}He), u_{10} is the wind speed in meters per second at a height of 10 m above the sea surface, $C_{i,eq}$ is the concentration of the gas at equilibrium (mol m^{-3}), and $C_{i,w}$ is the concentration of the gas in the water (mol m^{-3}). For QuikSCAT winds, $\gamma_G = 0.97$, and for NCEP winds $\gamma_G = 0.7$.

The flux of ^{3}He (or other gas) due to completely trapped bubbles was calculated as

$$F_C = 9.1 \times 10^{-11} (u_{10} - 2.27)^3 \frac{P_{i,a}}{RT}, \qquad (3)$$

where $P_{i,a}$ is the partial pressure of the gas (i.e., ^{3}He) in the atmosphere calculated from the fractional abundance of the gas and the variable total atmospheric pressure (Pa), R is the gas constant (8.31 m^3 Pa mol^{-1} K^{-1}), and T is the temperature (K).

The flux of ^{3}He (or another gas) (in units of mol m^{-3} s^{-1}) due to partially trapped bubbles was calculated as

$$F_P = 2.2 \times 10^{-3} \times (u_{10} - 2.27)^3 \alpha_i \left(\frac{D_i}{D_o}\right)^{\frac{2}{3}} \frac{(P_{i,b} - P_{i,w})}{RT}, \qquad (4)$$

where α is the Bunsen solubility coefficient of the gas (Benson and Krause, 1980, for ^{3}He), D_i is the diffusivity coefficient (for ^{3}He determined with the fractionation factor from Bourg and Sposito (2008) and the diffusivity coefficient of Jahne, 1987), D_o is a normalization factor equal to 1 which is included in order to simplify the units (m^2 s^{-1}), $P_{i,b}$ is the pressure of the gas in the bubble (Pa), and $P_{i,w}$ is the partial pressure of the gas in the water (Pa).

$P_{i,b}$ is approximated by

$$P_{i,b} = X_i \left(P_{atm} + \rho g z_{bub}\right), \qquad (5)$$

where X_i is the mole fraction of the gas in dry air, P_{atm} is the atmospheric pressure of dry air (Pa), ρ is the density of water (kg m^{-3}), g is the gravitational acceleration (9.81 m s^{-2}), and z_{bub} is the depth to which the bubble sinks (m), which is parameterized according to Graham et al. (2004):

$$z_{bub} = (0.15 \cdot u_{10} - 0.55). \qquad (6)$$

The main numbers reported in this paper (i.e., the total nitrate flux of 0.65 mol m^{-2} yr^{-1}) were calculated using the S09 parameterization as described above by Eqs. (2) to (6) since it was derived from a noble gas time series collected concurrently with the helium isotope data used in this study. Thus, since samples were collected at the same location and time,

S09 is based on exactly the same physical conditions (wind range, temperature range, etc.) as experienced by the helium isotopes. We explored the consequence of using other gas exchange parameterizations that explicitly include bubbles, namely the Nicholson et al. (2011) (subsequently referred to as N11) parameterization and the Liang et al. (2013) parameterization (subsequently referred to as L13). N11 is based on a global inversion of deep N_2, Ar, N_2 / Ar, and Kr / Ar data and thus reflects a larger perspective on gas exchange though perhaps one not quite as suitable to this specific study. N11 has a similar formulation for air injection to S09 although N11 does not include the effect of the partial pressure difference between enhanced pressure in the bubbles and pressure in the water when determining the flux due to partially trapped bubbles. L13 is based on a mechanistic model that explicitly includes the bubble size spectrum.

Calculations of the dynamic solubility equilibrium and the flux of ^{3}He were also made using NCEP reanalysis winds instead of QuikSCAT winds. When NCEP reanalysis winds were used in the model, the gas exchange parameterization of Stanley et al. (2009b) was modified to a parameterization that was calculated using NCEP winds. For example, the gas exchange scaling factor, γ_G, is 0.97 when using QuikSCAT winds (as reported in Stanley et al., 2009b) but is only 0.7 using NCEP winds.

The ^{3}He flux, calculated from Eq. (1), is then corrected for the flux of ^{3}He due to in situ tritium decay ($F_{HeFromTrit}$):

$$F_{HeCorr} = F_{He} - F_{HeFromTrit}. \qquad (7)$$

$F_{HefromTrit}$ is calculated by using the radioactive decay equation ($A = N\lambda$, where A is activity of ^{3}He, N is the number of atoms of tritium, and λ is half-life of tritium), the half-life of tritium ($\lambda = 12.31$ years), and the mixed-layer tritium concentrations measured concurrently with the ^{3}He data presented in this study. This yields a flux of ^{3}He produced in numbers of moles per cubic meter. We then multiply this flux by 300 m to calculate a flux in units of moles per square meter for the ^{3}He produced by tritium decay in the upper 300 m of the ocean. This flux equals roughly 15 % of the total ^{3}He flux calculated from Eq. (1) and is subtracted from the total ^{3}He flux to yield the ^{3}He flux that must be supported by vertical transport (Eq. 7).

The nitrate flux (F_{NO_3}) was then calculated as the product between the corrected ^{3}He flux and the nitrate : ^{3}He ratio (R):

$$F_{NO_3} = F_{HeCorr} \times R. \qquad (8)$$

The ratio R was calculated by determining the slope of a type II regression of NO_3 vs. ^{3}He for samples measured in the upper 400 m of water during the 3-year time series ($N = 218$). Only data with [NO_3] > 2 μmol kg^{-1} were used in the regression since water with NO_3 concentration below this threshold represents water in the euphotic zone where ^{3}He and NO_3 are decoupled. Jenkins and Doney (2003) studied the effect of using different data for the NO_3 : ^{3}He correlation – data
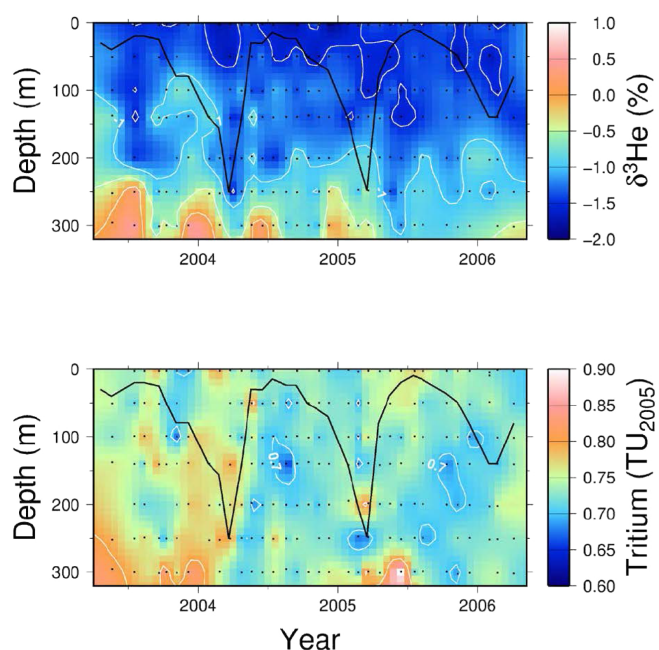

Figure 1. A time series of helium isotope ratio anomaly (in percent) relative to the atmospheric ^{3}He / ^{4}He ratio (upper panel) and tritium (in tritium units) decay corrected to January 2005 (lower panel) at the Bermuda Atlantic Time-series Site in the North Atlantic near Bermuda. Sampling, designated by black dots, was approximately monthly over the $\sim$ 3-year period. The black line is the mixed-layer depth estimated from the CTD (conductivity, temperature, depth) data.

based on vertical correlation (as here), on density surfaces, or at base of the winter mixed layer – and found that the slopes were similar no matter which data set was used.

3 Results and discussion

3.1 The fluxes of helium-3 and nitrate

The ^{3}He and tritium data collected in this study between 2003 and 2006 are presented in Fig. 1. The gradient of ^{3}He with depth is clearly visible. In contrast, tritium has a more uniform distribution with depth in the upper 300 m. The lack of excess ^{3}He in the mixed layer (mixed layer is demarcated by the thick black line) is because of air–sea gas exchange, which results in a flux of excess ^{3}He out of the ocean into the atmosphere. This sustained air–sea gas exchange results in a decreasing inventory of tritiugenic ^{3}He in the ocean over time. Multiple measurements within the mixed layer were averaged in order to calculate the mixed-layer concentrations of ^{3}He (Fig. 2a). The dynamic solubility equilibrium (blue curve on Fig. 2a) is significantly smaller than the ^{3}He concentrations, resulting in a sea-to-air flux of ^{3}He (Fig. 2c).
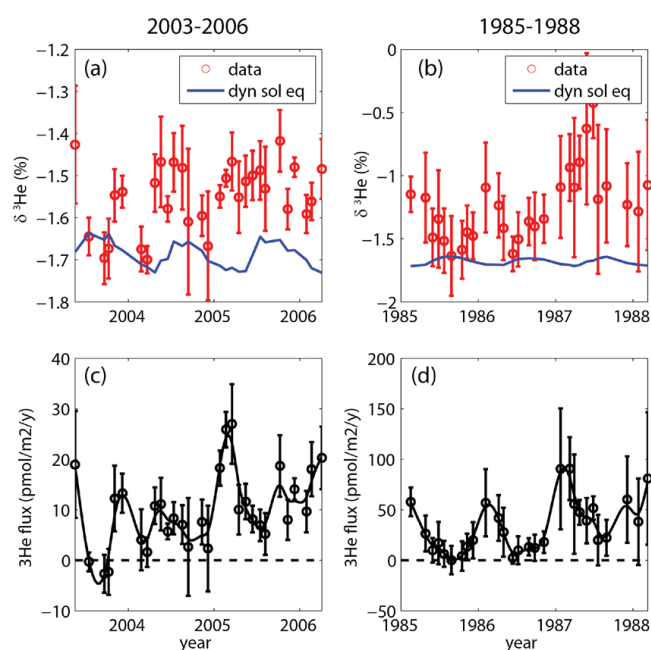
Figure 2. Mixed-layer δ^3He data from **(a)** 2003 to 2006 and **(b)** 1985 to 1988 as well as the dynamic solubility equilibrium for δ^3He. Error bars represent standard error of multiple measurements within the mixed layer. Fluxes of ^{3}He calculated from the data for **(c)** 2003–2006 and **(d)** 1985–1988. Note the difference in scales on the y axes for the two time periods.

Additionally, since we now have a better understanding of the dynamic solubility equilibrium, both because of the extensive information on gas exchange garnered from the noble gases and because of more accurate estimates of molecular diffusivity of ^{3}He, we have also recalculated the ^{3}He and nitrate fluxes for the data from 1985 to 1988 that were originally presented in Jenkins and Doney (2003). Thus, the ^{3}He concentrations from 1985 to 1988 as well as the dynamic solubility equilibrium for that time period are presented in Fig. 2b. Note the difference of scales in Fig. 2a and b. There is much less ^{3}He in 2003–2006 than in the 1980s because of a decreased ^{3}He source in the thermocline due to tritium decay over time and decades of outgassing of ^{3}He.

The average ^{3}He flux, corrected for tritium ingrowth, over the 2003–2006 time period is calculated to be $7.9 \pm 1\,\mathrm{pmol\,m^{-2}\,yr^{-1}}$ (Table 1). The flux due to tritium ingrowth in the mixed layer, determined using the average tritium concentration and considering tritium that could be accessed in the upper 300 m of the ocean, was $1.2 \pm 0.1\,\mathrm{pmol\,m^{-2}\,yr^{-1}}$ during this period. The integrated ^{3}He flux is multiplied by a $NO_3 : {}^3$He ratio of $82.9 \times 10^9 \pm 2 \times 10^9\,\mathrm{mol\ NO_3\ mol^{-1}\ {}^3He}$ (Fig. 3) in order to calculate a NO_3 flux of $0.65 \pm 0.14\,\mathrm{mol\ N\,m^{-2}\,yr^{-1}}$. The nitrate flux calculated by the flux gauge method used here represents the lower bound of new production in the northern half of the subtropical gyre. It represents a lower bound

estimate because it only includes the new production based on the upward physical transport of nutrients. It does not include any new production due to nitrogen fixation, zooplankton migration, or atmospheric deposition of nitrate. At BATS, nitrogen fixation has been estimated to be 0.03 to 0.08 mol $\mathrm{N\,m^{-2}\,yr^{-1}}$ (Singh et al., 2013; Knapp et al., 2008), which is equivalent to 5 to 12 % of the new production we report from the flux gauge method. Zooplankton migration from 2003 to 2006 has been estimated to support a new production of 2 g $\mathrm{C\,m^{-2}\,yr^{-1}}$ (Steinberg et al., 2012), which is equivalent to $0.025\,\mathrm{mol\ N\,m^{-2}\,yr^{-1}}$ using the revised Redfield ratios of Anderson and Sarmiento (1994) and thus is only 4 % of the new production rate estimated by the flux gauge technique. Estimates of the nitrate supply due to atmospheric deposition range from 0.006 mol N to $0.026\,\mathrm{mol\ N\,m^{-2}\,yr^{-1}}$ (Singh et al., 2013; Knapp et al., 2010), thus being at most 4 % of the new production flux estimated here from the flux gauge method. Thus, in total, the sources of new nitrate that are not accounted by the flux gauge method may mean that the new production estimate given here is only about 80 % to 85 % of the total new production rate. The flux estimate represents the northern half of the gyre – rather than just the BATS site – because the water in the thermocline that is vertically transported at the BATS site originates from the northern half of the gyre (Talley, 2003).

The nitrate fluxes calculated with the NCEP wind-derived ^{3}He fluxes are very similar to those calculated by QuikSCAT winds (Table 1). This is because the gas exchange parameterizations we used to calculate the flux from the ^{3}He concentration data and to calculate the dynamic solubility equilibrium were separately tuned to observed noble gas data for QuikSCAT and NCEP. We were able do this since we had the wealth of noble gas data collected concurrently, allowing for a good model of air–sea gas exchange with two different wind products.

3.2 Uncertainties and sensitivity studies

There are a number of sources of uncertainty in the estimate of nitrate fluxes from the helium flux gauge technique. Here we describe these uncertainties and the results of sensitivity studies examining the effect of the sources of error. Table 2 lists the main sources of uncertainty in the calculations. One of the largest sources of uncertainty is uncertainty in the gas transfer velocity k (Eq. 1). Stanley et al. (2009b) illustrate how the time series of noble gases collected concurrently with this data results in uncertainties of 14 % in the gas transfer velocity k. Since k is directly used to calculate the ^{3}He air–sea flux from the difference between measured ^{3}He concentration and dynamic solubility equilibrium, this uncertainty directly translates into a 14 % uncertainty in ^{3}He flux and ultimately in nitrate flux.

The second largest uncertainty in the nitrate flux is the uncertainty in the dynamic solubility equilibrium caused by uncertainties in the parameterization of air injection.

Table 1. Fluxes calculated from the flux gauge technique for two different time periods. 1σ uncertainty estimates for each flux are given in parentheses underneath the reported value for each quantity.

Time period	NO$_3$: ^{3}He $\times 10^{-3}$ (μmol pmol^{-1})	QuikSCAT winds		NCEP winds	
		^{3}He Flux (pmol m^{-2} yr^{-1})	NO$_3$ flux (mol m^{-2} yr^{-1})	^{3}He flux (pmol m^{-2} yr^{-1})	NO$_3$ flux (mol m^{-2} yr^{-1})
2003–2006	82.9 (2.1)	7.9 (1.7)	0.65 (0.14)	8.3 (1.8)	0.69 (0.15)
1985–1988	34.5 (1.1)	– –	– –	30.4 (5.4)	1.05 (0.2)

Table 2. The fractional uncertainty caused by different sources in the calculations of nitrate flux for the 2003–2006 time period.

Source of error	% uncertainty	Reference or method
Air–sea gas exchange	14 %	Stanley et al. (2009)
Dynamic solubility equilibrium		
– From diffusivity	10 %	Calculated with range from Bourg and Sposito (2008)
– From bubble treatment	13 %	Calculated with range of gas exchange from Stanley et al. (2009)
Measurement error	5 %	Integration of error at each time point
NO$_3$: ^{3}He slope	2.5 %	Type 2 regression
Tritium correction	1 %	Tritium measurement uncertainty propagated to ^{3}He flux

Three different parameterizations of air injection were used (see Sect. 2.2) in order to investigate the robustness of the flux gauge number with respect to air injection. The nitrate fluxes determined using these three different parameterizations when calculating the dynamic solubility equilibrium are 0.65 with S09, 0.55 with N11, and 0.48 mol m^{-2} yr^{-1} with L13. The standard deviation of these three numbers (0.08 mol m^{-2} yr^{-1} = 13 % of reported nitrate flux) is used as a measure of the uncertainty due to air injection. The S09 value was used for reporting the "base case" number (i.e., the number reported in the abstract and the conclusion) because S09 is based on data collected at the same time and location as the ^{3}He data used in this study and thus is likely to reflect gas exchange best in these conditions. Notably, the root mean square deviation between observed helium surface saturation anomalies and the saturation anomalies predicted by the PWP model run with either the S09 or N11 parameterization is the same (1.3 %). The root mean square deviation, however, for the model–data fit of the L13 parameterization is almost double that (2.5 %), suggesting that L13 does not represent air injection at this location and time as well as S09 or N11. The root mean square deviation between model and data for surface saturation anomalies for all the other stable noble gases (Ne, Ar, Kr, and Xe) agrees better for S09 and N11 than for L13 though the difference becomes smaller for the heavier gases – i.e., the L13 model matches observed data almost as well for Kr or for Xe as does S09 or N11. Since the

L13 model does not match the surface saturation anomalies of He as well as S09 or N11 (i.e., double the RMSD), L13 is probably not a good model to use for air injection in this study, and thus calculating the uncertainty from the standard deviation of fluxes determined when using all three gas exchange parameterization leads to a conservative estimate of the total uncertainty due to air injection. We also examined the effect on the nitrate flux of using different sets of air injection parameters from the S09 parameterization. Specifically, we use many of the parameter sets determined in Table 1 of Stanley et al. (2009b), including the sets of parameters determined for different physical parameters in the model and different weightings of the cost function. We found that the dynamic solubility equilibrium changed by only a small amount in these scenarios so that the overall standard deviation of the ^{3}He flux for all the different scenarios of S09 was only 2 %.

The third-largest source of uncertainty in the nitrate flux is the uncertainty in the determination of the dynamic solubility equilibrium due to uncertainties in the molecular diffusivity of ^{3}He with respect to ^{4}He. The dynamic solubility equilibrium is sensitive to the molecular diffusivity due to the relative diffusive gas exchange of ^{3}He vs. ^{4}He (i.e., Schmidt number dependence) and due to the effect of the air injection of partially trapped bubbles – during air injection, ^{3}He diffuses more quickly out of the bubbles than ^{4}He. We ran sensitivity studies with the range of molecular diffusivities estimated by Bourg and Sposito (2008) and found that
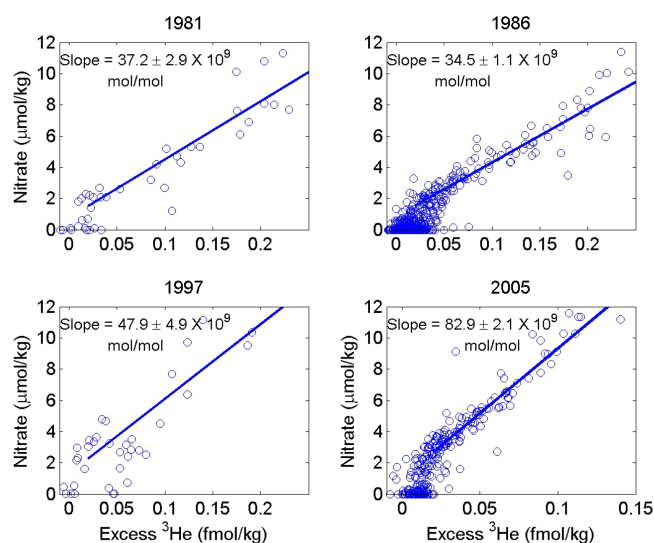
Figure 3. The observed relationship between excess (tritiugenic) ^{3}He and dissolved inorganic nitrate near Bermuda at four points in time. The 1986 and 2005 relations are based on approximately 3-year time series occupations near Bermuda (the former at Hydrostation S and the latter at BATS). The 1981 and 1997 data sets are from cruise stations within ~ 500 km of the site. Only samples with potential density anomalies less than 26.8 kg m^{-3} are plotted and used. Note the "waterfall" effect at low ^{3}He and nitrate concentrations in the euphotic zone, where the two tracers become uncoupled due to differing boundary conditions. The straight lines, from which the slopes are obtained, are type II linear regressions of points with nitrate concentrations in excess of 2 µmol kg^{-1}. The lower bound nitrate limit was chosen to avoid the tracer-decoupled points.

the ^{3}He flux changed by ±10 % depending on the molecular diffusivities used. Although experiments with helium isotopes have not yet been performed to confirm the diffusivities predicted by Bourg and Sposito (2008), two separate experimental studies (Tempest and Emerson, 2013; Tyroller et al., 2014) have shown good agreement with the Ne isotope diffusivities calculated by Bourg and Sposito (2008), giving us confidence in the Bourg and Sposito (2008) helium predictions.

The effect of the measurement error of ^{3}He is a smaller uncertainty than the systematic uncertainties listed above but does lead to an error of 5 % when propagated through all the calculations. Interestingly, for the 1985–1988 period, the absolute ^{3}He concentrations were much higher but the measurement uncertainty at that time was much worse, resulting in a similar 5 % contribution of measurement uncertainty during that period as well.

Uncertainties in the slope of NO$_3$: ^{3}He feed directly into uncertainty in the nitrate flux, resulting in a 2.5 % uncertainty in the nitrate flux. The uncertainties were derived from the uncertainty associated with the calculation of the slope using a type II regression and appropriate measurement uncertainties for the individual data points. Additional error in the

^{3}He flux – and thus propagated to the nitrate flux – comes from the correction for tritium ingrowth in the water column. However, since the ^{3}He flux due to in situ tritium production is relatively small (15 % of the total ^{3}He flux), the uncertainty on that number only contributes to a small fraction of the total uncertainty in the helium and nitrate fluxes (1 %).

3.3 Comparison to 1980s fluxes

The estimated nitrate flux for the period between 1985 and 1988 is 50 % larger than the nitrate flux for the 2003–2006 period, though over half of this difference can be accounted for by uncertainties in the flux estimates. For 1985–1988, our recomputed nitrate flux estimate is 1.05 ± 0.2 mol N m^{-2} yr^{-1} (Table 1), which is 25 % larger than the nitrate flux calculated for the same time period in Jenkins and Doney (2003). This difference between the 1985–1988 fluxes calculated here and those calculated in Jenkins and Doney (2003) stems from this calculation using a well-modeled dynamic solubility equilibrium. In the earlier study, we did not have the other noble gas data nor updated estimates of molecular diffusivity (Bourg and Sposito, 2008) and thus employed a simpler and likely less accurate estimate of the dynamic solubility equilibrium.

It is interesting to note that although the nitrate flux in 1985–1988 is only 50 % larger than the nitrate flux in 2003–2006, the ^{3}He flux in 1985–1988 is 300 % larger than the ^{3}He flux in 2003–2006. This is because in the 1980s, there was a much larger tritium inventory and consequently larger concentrations of ^{3}He in the main thermocline (Fig. 4). However, the slope of the NO$_3$: ^{3}He relationship also changes with time. The distribution of nutrients in the main thermocline is in an approximate steady state established by a balance between nutrient release by in situ remineralization of organic material and removal by physical processes related to ventilation, advection, and mixing. The corresponding thermocline distribution of tritiugenic ^{3}He is evolving as a transient tracer. Over time, as the bomb-tritium pulse penetrates the thermocline, the resultant ^{3}He maximum deepens and broadens (Jenkins, 1998). Consequently the relationship between ^{3}He and nutrients changes with time. Figure 3 is a plot of the NO$_3$: ^{3}He relationship for the upper 500 m of the water column near Bermuda at four points in time. Notably, the slope of the NO$_3$: ^{3}He relationship has increased by over a factor of 2 in the approximately 25 years spanned by this data.

While the nitrate flux is broadly similar between the two time periods, there is still a 50 % difference with the flux being larger in 1985–1988 than in 2003–2006. What can account for this difference? It is not because of NCEP winds being used in the 1985–1988 calculation and QuikSCAT winds being used in the 2003–2006 calculation because even if we do the 2003–2006 calculation with NCEP winds, we still get a 40 % difference between the flux in the two different decades (Table 1). It also is not likely to be due to the 1985–1988 data being from Hydrostation S, whereas the 2003–

2006 data are from BATS. Those two sites are only 28 km apart and since the ^{3}He flux gauge estimate is reflection of a much broader region, the relatively small difference in locations of samples likely does not play a role. It could be, in part, due to a time lag between the evolving subsurface $NO_3 : {}^3$He ratio and surface fluxes. Most likely, however, it is due to a real elevation in new production in the late 1980s compared to the 2003–2006 period. Winter mixed layers in the two time periods are similar, with the exception of a shallower than typical winter mixed-layer depth in 1986, and thus the difference in time periods is not likely an explanation for the difference in production between the periods.

Lomas et al. (2010) observed significant changes in export production at BATS over time, with the period between 1988 and 1995 having lower export fluxes than the period from 1995 to 2008. They attributed these changes to a shift in the North Atlantic Oscillation (NAO) from positive in the 1988–1995 period to neutral in the 1996–2008 period. Our older data are from 1985 to 1988 and were not included in the Lomas et al. (2010) study. The winter NAO index (JFM), which has been shown to be most sensitive to changes in subtropical mode water formation (Billheimer and Talley, 2013) and primary production (Lomas et al., 2010), was −1.2, 0.2, and −1.1 for 1985, 1986, and 1987, respectively. It was −0.3, −0.5, and −0.6 for 2004, 2005, and 2006 respectively. According to Lomas et al. (2010), a more negative winter NAO, as was mostly seen in the 1985–1988 period, would be associated with higher production, which is indeed what we found in this study.

A more negative NAO is usually correlated with a greater production of subtropical mode waters (STMW) via enhanced surface buoyancy loss and vertical convection (Billheimer and Talley, 2013). Indeed, estimates of Kelly and Dong (2013) suggest that there was increased formation of STMW in 1985–1988 compared to 2003–2006. We thus find that higher rates of new production are associated with time periods of a higher generation of STMW. This is in contrast to the hypothesis of Palter et al. (2005), who suggested that increased STMW production would lead to a reduction in primary production due to decreased nutrients below the mixed layer in the vertically homogenized mode water region since the decreased nutrients would lead to a smaller nutrient supply from the main thermocline below the mode water region and thus to smaller rates of primary production.

The highest annual flux in the 1985–1988 period comes from 1987 (Fig. 2d). Interestingly, while the NAO index of 1987 was similar to that of 1985 and 2003–2006, the NAO index of 1986 was positive. It has been shown that chlorophyll correlates better with the NAO index at BATS using a 1-year time lag (Cianca et al., 2012). Thus, potentially, the higher fluxes we see in 1987 are a result of the higher NAO index in 1986. However, this would run counter to the general trend suggested by Lomas et al. (2010) and seen in the rest of our data of higher rates of production with more negative NAO indices.
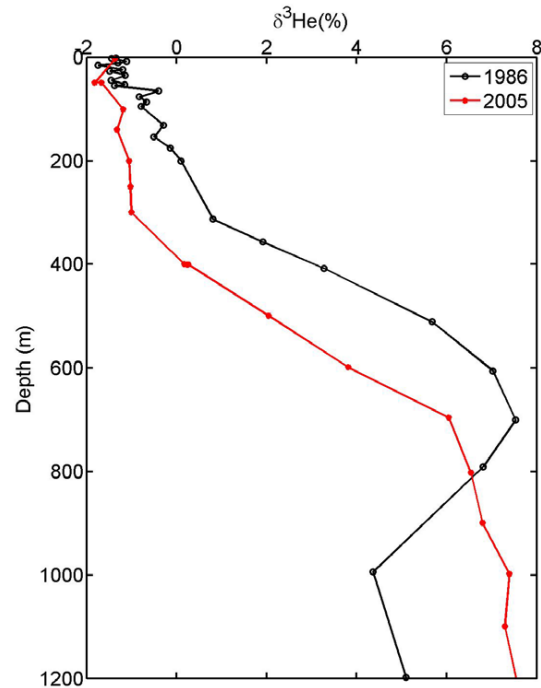

Figure 4. Representative profiles of δ^3He in the upper 1200 m of the water column in 1986 (black) and 2003–2006 (red). The profiles illustrate that in 1986 there was much higher δ^3He in the main thermocline and a larger gradient between the thermocline and the mixed layer than there was in 2006. This drives the observed greater ^{3}He flux in the 1980s compared to the 2000s.

3.4 Seasonal cycle

A seasonal cycle in ^{3}He flux is observed in both the 1985–1988 time period and the 2003–2006 time period (Fig. 5). The ^{3}He fluxes are highest in wintertime when the deep winter mixed layers at BATS draw water from the seasonal thermocline, bringing up higher amounts of ^{3}He and nitrate. But even in the summer, there is an upward flux of ^{3}He, suggesting an upward flux of nitrate. There is no observable nitrate in the summer mixed layer at BATS (Michaels et al., 1994; Steinberg et al., 2001), likely because the organisms consume all the nitrate as soon as it enters the euphotic zone. Thus the lack of observable nitrate, long known at BATS, does not mean that nitrate was never there. Hence the "paradox" of how summertime production can be supported at BATS without observable nutrients is in some sense answered by this clear sign that there is an upward nutrient flux, even in the summer. This supports the recent finding of Fawcett et al. (2014) showing evidence of nitrate supply to the mixed layer at BATS even in the summer.
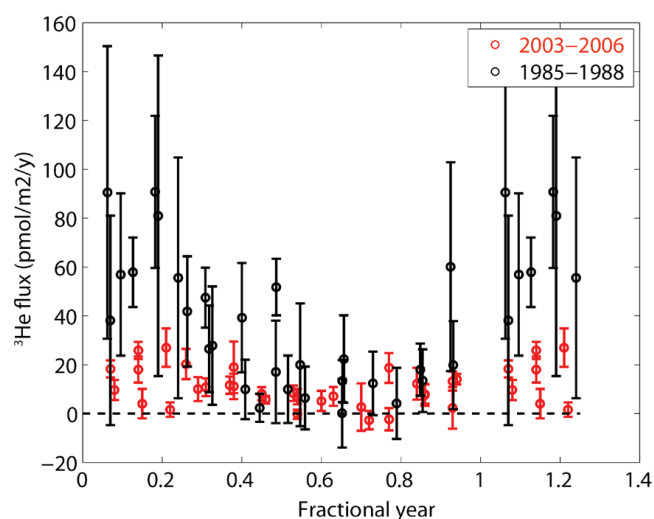
Figure 5. The ^{3}He flux as a function of fractional year for the 2003–2006 time period (red) and the 1985–1988 time period (black). The time period between 0 and 0.4 has been replicated from 1 to 1.4 in order to better visualize a seasonal cycle.

3.5 Comparison to other rates of biological productivity at BATS

The rate of new production estimated by the helium flux gauge technique presented in this study is larger than most of the rates of new production, net community production, or export production at BATS derived from other geochemical tracer approaches. Over long periods of time and on long spatial scales, new production, net community production, and export production should be equal (Dugdale and Goering, 1967). In carbon units, using the revised Redfield ratio of Anderson and Sarmiento (1994) of 106 : 16, new production estimated in this study was 4.3 ± 0.9 mol C m^{-2} yr^{-1} in 2003–2006 and 6.96 ± 1.3 mol C m^{-2} yr^{-1} in 1985–1988. Because of global and regional variations in the C : N ratio (Lomas et al., 2013; Martiny et al., 2013; Ono et al., 2001), there are additional uncertainties when converting nitrate fluxes to carbon fluxes. Additionally, as noted above, these rates represent new production derived from the physical vertical supply of nitrate over the northern half of the subtropical gyre.

Export fluxes as estimated by apparent oxygen utilization rates (AOUR) also represent fluxes over a similar northern region (Jenkins, 1980). Tritium samples were collected and used in conjunction with ^{3}He and O$_2$ data from the same cruises in 2003–2006 that the ^{3}He data in this paper come from to estimate apparent oxygen utilization rates (Stanley et al., 2012). The AOUR values were integrated to 500 m to yield a lower bound on annual export from the remineralization and oxygen consumption between 200 and 500 m of 2.1 ± 0.5 mol C m^{-2} yr^{-1}. Thus, the fluxes estimated by the helium flux gauge technique are nearly a factor of 2 greater

than the fluxes by AOUR, even though both represent a large geographical region.

A more local estimate of production comes from the seasonal drawdown of DIC (dissolved inorganic carbon) at BATS or from seasonal accumulation of O$_2$ with respect to Ar. Both techniques rely on the fact that photosynthesis produces O$_2$ and consumes CO$_2$, whereas respiration produces CO$_2$ and consumes O$_2$. Thus, the seasonal changes in O$_2$ or CO$_2$ constrain the net balance between photosynthesis and respiration. On the same cruises on which data for ^{3}He flux gauge technique were collected, the seasonal accumulation of O$_2$ and Ar was measured and used to estimate the rates of net community production of 1.2 to 2.4 mol C m^{-2} yr^{-1} (Stanley, 2007). Notably, this rate is similar to that of the AOUR estimate and a factor of 2 smaller than the ^{3}He flux gauge estimate. The seasonal accumulation of oxygen and argon has been used at other time periods to estimate the rate of net community production at BATS to be 2.2 to 3 mol C m^{-2} yr^{-1} (Spitzer and Jenkins, 1989; Luz and Barkan, 2009). Seasonal drawdown of DIC directly as well as the change in isotopic composition of ^{13}C of DIC have been used to estimate annual net community production fluxes of 1.7 to 4.9 mol C m^{-2} yr^{-1} (Gruber et al., 1998; Brix et al., 2006; Fernandez-Castro et al., 2012). The upper end of this range approximates the rate of new production we find here using the flux gauge technique. Interestingly, the DIC drawdown and O$_2$ / Ar approaches reflect a smaller spatial scale than the AOUR estimates but, at least in some cases, agree better with the ^{3}He flux gauge approach.

On even smaller spatial and temporal scales, ^{234}Th has been used to estimate export fluxes at BATS, resulting in rates of export production calculated to be 0.3 to 0.8 mol C m^{-2} yr^{-1} (Maiti et al., 2009) These fluxes are much smaller than the fluxes estimated by other geochemical tracers, which may in part be due to the fact that the ^{234}Th technique does not include the contribution of export due to DOC, whereas the other geochemical techniques do. DOC export in the Sargasso Sea has been estimated to be up to 1 mol C m^{-2} yr^{-1} (Hansell et al., 2012).

Why is the helium flux gauge technique yielding rates of new production at the high end of the range of rates from other geochemical tracers? In part this may be due to the broader spatial coverage of the flux gauge technique, but that is not enough to explain fully the discrepancy since the AOUR technique has a similar spatial area but smaller fluxes. One reason may be that ^{3}He and NO$_3$ are decoupled during obduction in the northern part of the gyre. The northwest Sargasso Sea, where the warm waters of the Gulf Stream leave the North American continent, is characterized by large latent heat fluxes and substantial downstream winter mixed-layer deepening (Worthington, 1972). In effect, upper thermocline isopycnals outcrop, a process referred to as obduction (Qiu and Huang, 1995). This outcropping brings remineralized nutrients and tritiugenic ^{3}He back to the seasonal layer. Whereas the time constant associated with nutrient re-

moval by biological processes is a matter of days, the exchange timescale for tritiugenic ^{3}He loss to the atmosphere from a deep mixed layer may be several weeks. In this respect the nutrients may have been removed, while the ^{3}He "signal" may persist, so the ^{3}He flux gauge may measure not only local new production but may also hold a more "regional" memory of the upstream, previous winter's production.

There are two approaches to estimating this obduction flux of ^{3}He. Given that they are rather crude in nature and involve rather different assumptions and, more importantly, scales, exact congruence would be unlikely. All that one can examine is whether they are broadly compatible with the fluxes obtained in this study. One way is to compute the eastward transport of ^{3}He through 52° W in the upper 300 m. Using the 2003 CLIVAR (Climate and Ocean: Variability, Predictability and Change) A20 section and geostrophic velocities relative to 200 dbar (data are publicly available from http://cchdo.ucsd.edu) (Jenkins and Stanley, 2008), the peak transport south of 38° N is 1.4 µmol s^{-1}. When this transport is averaged over the area of the northern half of the Sargasso Sea (approximately 3×10^6 km^2), this corresponds to a flux of ~ 0.5 amol m^{-2} s^{-1} or ~ 15 pmol m^{-2} yr^{-1} in 2003. The second calculation is based on the work of Qiu and Huang (1995), who estimated an obduction rate ranging from 50 to 250 m yr^{-1} in the northern Sargasso Sea (their Fig. 7f). Typical excess ^{3}He concentrations range from 0.02 to 0.04 pmol m^{-3} at 300 m depth, so one infers an upward ^{3}He flux ranging from 1 to 10 pmol m^{-2} yr^{-1}. The ^{3}He flux determined in this study is 7.9 pmol m^{-2} yr^{-1} and thus fits within the range of estimates of flux due to obduction.

4 Conclusions

In summary, we have used the approach of Jenkins and Doney (2003) to calculate the *physical* supply of subsurface nitrate to the euphotic zone at BATS as being 0.65 ± 0.14 mol m^{-2} yr^{-1}. This flux may support the new production of approximately 4.3 ± 0.9 mol C m^{-2} yr^{-1} due to the upward flux of nutrients over a broad region of the subtropical northwestern Atlantic. This reflects a lower bound on total new production since nitrate may come from other sources (nitrogen fixation, vertical migration, etc.) and thus this estimate may be underestimating total new production by 15 %. We show that the rates are consistent with, but lower than, rates of new production recalculated from similar data from 1985 to 1988 and that this difference may be related to subtropical mode water formation. We also show that the rates estimated by this technique are higher than most other rates of new production estimated at the BATS site. This work thus shows that upward flux of nutrients – even if not directly observed at BATS by traditional techniques – is more than sufficient to support the observed rates of net community production and export production calculated at BATS.

References

Anderson, L. A. and Sarmiento, J. L.: Redfield ratios of remineralization determined by nutrient data-analysis, Global Biogeochem. Cy., 8, 65–80, 1994.

Benson, B. B. and Krause Jr., D., : Isotopic fractionation of helium during solution: a probe for the liquid state, J. Solut. Chem., 9, 895–909, 1980.

Billheimer, S. and Talley, L. D.: Near cessation of Eighteen Degree Water renewal in the western North Atlantic in the warm winter of 2011–2012, J. Geophys. Res.-Oceans, 118, 6838–6853, 2013.

Bourg, I. C. and Sposito, G.: Isotopic fractionation of noble gases by diffusion in liquid water: Molecular dynamics simulations and hydrologic applications, Geochim. Cosmochim. Acta, 72, 2237–2247, 2008.

Brew, H. S., Moran, S. B., Lomas, M. W., and Burd, A. B.: Plankton community composition, organic carbon and thorium-234 particle size distributions, and particle export in the Sargasso Sea, J. Mar. Res., 67, 845–868, 2009.

Brix, H., Gruber, N., Karl, D. M., and Bates, N. R.: On the relationships between primary, net community, and export production in subtropical gyres, Deep-Sea Res. Pt. II, 53, 698–717, 2006.

Broecker, W. S. and Peng, T. H.: The distribution of bomb-produced tritium and radiocarbon at GEOSECS station 347 in the eastern North Pacific, Earth Planet. Sci. Lett., 49, 453–462, 1980.

Buesseler, K. O.: Do upper-ocean sediment traps provide an accurate record of particle flux?, Nature, 353, 420–423, 1991.

Buesseler, K. O., Lamborg, C., Cai, P., Escoube, R., Johnson, R., Pike, S., Masque, P., McGillicuddy, D., and Verdeny, E.: Particle fluxes associated with mesoscale eddies in the Sargasso Sea, Deep-Sea Res. Pt. II, 55, 1426–1444, 2008.

Cianca, A., Godoy, J. M., Martin, J. M., Perez-Marrero, J., Rueda, M. J., Llinas, O., and Neuer, S.: Interannual variability of chlorophyll and the influence of low-frequency climate modes in the North Atlantic subtropical gyre, Global Biogeochem. Cy., 26, Gb2002, doi:10.1029/2010gb004022, 2012.

Doney, S. C., Glover, D. M., and Jenkins, W. J.: A model function of the global bomb-tritium distribution in precipitation, 1960–1986, J. Geophys. Res., 97, 5481–5492, 1992.

Dong, S. F. and Kelly, K. A.: How Well Do Climate Models Reproduce North Atlantic Subtropical Mode Water?, J. Phys. Oceanogr., 43, 2230–2244, 2013.

Dugdale, R. C. and Goering, J. J.: Uptake of new and regenerated forms of nitrogen in primary productivity., Limnol. Oceanogr., 12, 196–206, 1967.

Dugdale, R. C., Wilkerson, F. P., Barber, R. T., and Chavez, F. P.: Estimating new production in the equatorial Pacific Ocean at 150° W, J. Geophys. Res., 97, 681–686, 1992.

Fawcett, S. E., Lomas, M. W., Ward, B. B., and Sigman, D. M.: The counterintuitive effect of summer-to-fall mixed layer deepening on eukaryotic new production in the Sargasso Sea, Global Biogeochem. Cy., 28, 86–102, 2014.

Fernandez-Castro, B., Anderson, L., Maranon, E., Neuer, S., Ausin, B., Gonzalez-Davila, M., Santana-Casiano, M., Cianca, A., Santana, R., Llinas, O., Rueda, M. J., and Mourino-Carballido, B.: Regional differences in modelled net production and shallow remineralization in the North Atlantic subtropical gyre, Biogeosciences, 9, 2831–2846, doi:10.5194/bg-9-2831-2012, 2012.

Fuchs, G., Roether, W., and Schlosser, P.: Excess ^{3}He in the ocean surface layer, J. Geophys. Res., 92, 6559–6568, 1987.

Graham, A., Woolf, D. K., and Hall, A. J.: Aeration due to breaking waves. Part I: Bubble populations, J. Phys. Oceanogr., 34, 989–1007, 2004.

Gruber, N., Keeling, C. D., and Stocker, T. F.: Carbon-13 constraints on the seasonal inorganic carbon budget at the BATS site in the northwestern Sargasso Sea, Deep-Sea Res. Pt. II, 45, 673–717, 1998.

Hansell, D. A., Carlson, C. A., and Schlitzer, R.: Net removal of major marine dissolved organic carbon fractions in the subsurface ocean, Global Biogeochem. Cy., 26, Gb1016, doi:10.1029/2011gb004069, 2012.

Harrison, W. G. and Harris, L. R.: Isotope-Dilution and Its Effects on Measurements of Nitrogen and Phosphorus Uptake by Oceanic Microplankton, Mar. Ecol.-Prog. Ser., 27, 253–261, 1986.

Jahne, B., Heinz, G., and Dietrich, W.: Measurement of the diffusion coefficients of sparingly soluble gases in water, J. Geophys. Res., 92, 10767–10776, 1987.

Jenkins, W. J.: Tritium and He-3 in the Sargasso Sea, J. Mar. Res., 38, 533–569, 1980.

Jenkins, W. J.: Nitrate flux into the euphotic zone near Bermuda, Nature, 331, 521–523, 1988a.

Jenkins, W. J.: Nitrate flux into the euphotic zone near Bermuda, Nature, 331, 521–523, 1988b.

Jenkins, W. J.: The use of anthropogenic tritium and 3He to study subtropical gyre ventilation and circulation, Philos. Tr. Soc. A(London), 325, 43–61, 1988c.

Jenkins, W. J. and Doney, S. C.: The subtropical nutrient spiral, Global Biogeochem. Cy., 17, 1110, doi:10.29/2003GB002085, 2003.

Jenkins, W. J. and Goldman, J. C.: Seasonal oxygen cycling and primary production in the Sargasso Sea, J. Mar. Res., 43, 465–491, 1985.

Jenkins, W. J. and Stanley, R. H. R.: The Helium-3 flux gauge in the subtropical North Atlantic: What does it tell us about nutrient fluxes and new production in an oligotrophic gyre?, Ocean Sciences Meeting, Orlando, FL, 2008.

Kalnay, E., Kanamitsu, M., Kistler, R., Collins, W., Deaven, D., Gandin, L., Iredell, M., Saha, S., White, G., Woollen, J., Zhu, Y., Chelliah, M., Ebisuzaki, W., Higgins, W., Janowiak, J., Mo, K. C., Ropelewski, C., Wang, J., Leetmaa, A., Reynolds, R., Jenne, R., and Joseph, D.: The NCEP/NCAR 40-year reanalysis project, Bullet. Am. Meteorol. Soc., 77, 437–471, 1996.

Kelly, K. A. and Dong, S.: The contributions of atmosphere and ocean to North Atlantic Subtropical Mode Water volume anomalies, Deep-Sea Res. Pt. II, 91, 111–127, 2013.

Knapp, A. N., DiFiore, P. J., Deutsch, C., Sigman, D. M., and Lipschultz, F.: Nitrate isotopic composition between Bermuda and Puerto Rico: Implications for N1 fixation in the Atlantic Ocean, Global Biogeochem. Cy., 22, Gb3014, doi:10.1029/2007gb003107, 2008.

Knapp, A. N., Hastings, M. G., Sigman, D. M., Lipschultz, F., and Galloway, J. N.: The flux and isotopic composition of reduced and total nitrogen in Bermuda rain, Mar. Chem., 120, 83–89, 2010.

Liang, J. H., Deutsch, C., McWilliams, J. C., Baschek, B., Sullivan, P. P., and Chiba, D.: Parameterizing bubble-mediated air-sea gas exchange and its effect on ocean ventilation, Global Biogeochem. Cy., 27, 894–905, 2013.

Lipschultz, F.: A time-series assessment of the nitrogen cycle at BATS, Deep-Sea Res. Pt. II, 48, 1897–1924, 2001.

Lipschultz, F., Bates, N. R., Carlson, C. A., and Hansell, D. A.: New production in the Sargasso Sea: History and current status, Global Biogeochem. Cy., 16, 1001, doi:10.1029/2000gb001319, 2002.

Lomas, M. W., Steinberg, D. K., Dickey, T., Carlson, C. A., Nelson, N. B., Condon, R. H., and Bates, N. R.: Increased ocean carbon export in the Sargasso Sea linked to climate variability is countered by its enhanced mesopelagic attenuation, Biogeosciences, 7, 57–70, doi:10.5194/bg-7-57-2010, 2010.

Lomas, M. W., Bates, N. R., Johnson, R. J., Knap, A. H., Steinberg, D. K., and Carlson, C. A.: Two decades and counting: 24-years of sustained open ocean biogeochemical measurements in the Sargasso Sea, Deep-Sea Res. Pt. II, 93, 16–32, 2013.

Lott, D. E. and Jenkins, W. J.: Advances in analysis and shipboard processing of tritium and helium samples, International WOCE Newsletter, 30, 27–30, 1998.

Luz, B. and Barkan, E.: Net and gross oxygen production from O-2/Ar, O-17/O-16 and O-18/O-16 ratios, Aq. Microb. Ecol., 56, 133–145, 2009.

MacMahon, D.: Half-life evaluations for ^{3}H, ^{90}Sr, and ^{90}Y, Appl.Radiat. Isotopes, 54, 1417–1419, 2006.

Maiti, K., Benitez-Nelson, C. R., Lomas, M. W., and Krause, J. W.: Biogeochemical responses to late-winter storms in the Sargasso Sea, III-Estimates of export production using Th-234 : U-238 disequilibria and sediment traps, Deep-Sea Res. Part I, 56, 875–891, 2009.

Maiti, K., Buesseler, K. O., Pike, S. M., Benitez-Nelson, C., Cai, P. H., Chen, W. F., Cochran, K., Dai, M. H., Dehairs, F., Gasser, B., Kelly, R. P., Masque, P., Miller, L. A., Miquel, J. C., Moran, S. B., Morris, P. J., Peine, F., Planchon, F., Renfro, A. A., van der Loeff, M. R., Santschi, P. H., Turnewitsch, R., Waples, J. T., and Xu, C.: Intercalibration studies of short-lived thorium-234 in the water column and marine particles, Limnol. Oceanogr. Meth., 10, 631–644, 2012.

Marra, J.: Approaches to the measurement of plankton production, Phytoplankton Productivity: Carbon Assimilation in Marine and Freshwater Ecosystems, edited by: Williams, P. J. L., Thomas, D. N., and Reynolds, C. S., Blackwell, Malden, MA, 31 pp., 2002.

Marra, J.: Net and gross productivity: weighing in with C-14, Aq. Microb. Ecol., 56, 123–131, 2009.

Martiny, A. C., Vrugt, J. A., Primeau, F. W., and Lomas, M. W.: Regional variation in the particulate organic carbon to nitrogen ratio in the surface ocean, Global Biogeochem. Cy., 27, 723–731, 2013.

Michaels, A. F., Bates, N. R., Buesseler, K. O., Carlson, C. A., and Knap, A. H.: Carbon system imbalances in the Sargasso Sea, Nature, 372, 537–540, 1994.

Nicholson, D., Emerson, S., and Khatiwala, S.: An inverse approach to estimate bubble-mediated air-sea gas flux from inert gas measurements, in: Proceedings of the 6th international symposium on gas transfer at water surfaces, edited by: Komori, S., Emerson, S., and Kurose, R., Kyoto University Press, Kyoto, Japan 2011..

Ono, S., Ennyu, A., Najjar, R. G., and Bates, N. R.: Shallow remineralization in the Sargasso Sea estimated from seasonal variations in oxygen, dissolved inorganic carbon and nitrate, Deep-Sea Res., 48, 1567–1582, 2001.

Ostlund, H. G., Dorsey, H. G., and Rooth, C. G.: GEOSECS North Atlantic Radiocarbon and Tritium Results, Earth Planet. Sci. Lett., 23, 69–86, 1974.

Owens, S. A., Buesseler, K. O., Lamborg, C. H., Valdes, J., Lomas, M. W., Johnson, R. J., Steinberg, D. K., and Siegel, D. A.: A new time series of particle export from neutrally buoyant sediments traps at the Bermuda Atlantic Time-series Study site, Deep-Sea Res. Part I, 72, 34–47, 2013.

Palter, J. B., Lozier, M. S., and Barber, R. T.: The effect of advection on the nutrient reservoir in the North Atlantic subtropical gyre, Nature, 437, 687–692, 2005.

Peterson, B. J.: Aquatic Primary Productivity and the C-14-CO_2 Method – a History of the Productivity Problem, Annu. Rev. Ecol. Syst., 11, 359–385, 1980.

Price, J. F., Weller, R. A., and Pinkel, R.: Diurnal cycling – observations and models of the upper ocean response to diurnal heating, cooling, and wind mixing, J. Geophys. Res.-Oceans, 91, 8411–8427, 1986.

Qiu, B. and Huang, R. X.: Ventilation of the North Atlantic and North Paciifc: subduction versus obduction, J. Phys. Oceanogr., 25, 2374–2390, 1995.

Rooth, C. G. and Ostlund, H. G.: Penetration of tritium into the North Atlantic thermocline, Deep-Sea Res., 19, 481–492, 1972.

Scarratt, M. G., Marchetti, A., Hale, M. S., Rivkin, R. B., Michaud, S., Matthews, P., Levasseur, M., Sherry, N., Merzouk, A., Li, W. K. W., and Kiyosawa, H.: Assessing microbial responses to iron enrichment in the Subarctic Northeast Pacific: Do microcosms reproduce the in situ condition?, Deep-Sea Res. Pt. II, 53, 2182–2200, 2006.

Singh, A., Lomas, M. W., and Bates, N. R.: Revisiting N-2 fixation in the North Atlantic Ocean: Significance of deviations from the Redfield Ratio, atmospheric deposition and climate variability, Deep-Sea Res. Pt. II, 93, 148–158, 2013.

Spitzer, W. S. and Jenkins, W. J.: Rates of vertical mixing, gas-exchange and new production – estimates from seasonal gas cycles in the upper ocean near Bermuda, J. Mar. Res., 47, 169–196, 1989.

Stanley, R. H. R., Jenkins, W. J., and Doney, S. C.: Quantifying seasonal air-sea gas exchange processes using noble gas time-series: A design experiment, J. Mar. Res., 64, 267–295, 2006.

Stanley, R. H. R., Baschek, B., Lott, D. E., and Jenkins, W. J.: A new automated method for measuring noble gases and their isotopic ratios in water samples, Geochem. Geophys. Geosys., 10, Q05008, doi:10.1029/2009GC002429, 2009a.

Stanley, R. H. R., Jenkins, W. J., Doney, S. C., and Lott III, D. E.: Noble Gas Constraints on Air-Sea Gas Exchange and Bubble Fluxes, J. Geophys. Res.-Oceans, 114, C11020, doi:10.1029/2009JC005396, 2009b.

Stanley, R. H. R., Doney, S. C., Jenkins, W. J., and Lott, III, D. E.: Apparent oxygen utilization rates calculated from tritium and helium-3 profiles at the Bermuda Atlantic Time-series Study site, Biogeosciences, 9, 1969–1983, doi:10.5194/bg-9-1969-2012, 2012.

Stark, S., Jenkins, W. J., and Doney, S. C.: Deposition and recirculation of tritium in the North Pacific Ocean, J. Geophys. Res., 109, C06009, doi:10.1029/2003JC002150, 2004.

Steinberg, D. K., Carlson, C. A., Bates, N. R., Johnson, R. J., Michaels, A. F., and Knap, A. H.: Overview of the US JGOFS Bermuda Atlantic Time-series Study (BATS): a decade-scale look at ocean biology and biogeochemistry, Deep-Sea Res. Pt. II, 48, 1405–1447, 2001.

Steinberg, D. K., Lomas, M. W., and Cope, J. S.: Long-term increase in mesozooplankton biomass in the Sargasso Sea: Linkage to climate and implications for food web dynamics and biogeochemical cycling, Global Biogeochem. Cy., 26, Gb1004, doi:10.1029/2010gb004026, 2012.

Stewart, G., Moran, S. B., Lomas, M. W., and Kelly, R. P.: Direct comparison of Po-210, Th-234 and POC particle-size distributions and export fluxes at the Bermuda Atlantic Time-series Study (BATS) site, J. Environ. Radioact., 102, 479–489, 2011.

Talley, L. D.: Shallow, intermediate, and deep overturning components of the global heat budget, J. Phys. Oceanogr., 33, 530–560, 2003.

Tempest, K. E. and Emerson, S.: Kinetic isotopic fractionation of argon and neon during air-water gas transfer, Mar. Chem., 153, 39-47, 2013.

Tyroller, L., Brennwald, M. S., Maechler, L., Livingstone, D. M., and Kipfer, R.: Fractionation of Ne and Ar isotopes by molecular diffusion in water, Geochim. Cosmochim. Acta, 136, 60–66, 2014.

Weiss, W. M. and Roether, W.: The rates of tritium input to the world oceans, Earth Planet. Sci. Lett., 49, 435–446, 1980.

Worthington, L. V.: Negative oceanic heat flux as a cause of watermass formation, J. Phys. Oceanogr., 2, 205–211, 1972.